Biomedicine & Pharmacotherapy 171 (2024) 116094

Contents lists available at ScienceDirect

Biomedicine & Pharmacotherapy

journal homepage: www.elsevier.com/locate/biopha

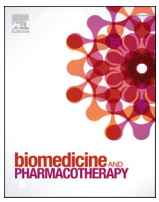

Oleoylethanolamide attenuates acute-to-chronic kidney injury: *in vivo* and *in vitro* evidence of PPAR-α involvement

Federica Comella [a], Adriano Lama [a], Claudio Pirozzi [a], Chiara Annunziata [a], Giuseppe Piegari [b], Federica Sodano [a], Stefania Melini [a], Orlando Paciello [b], Francisca Lago Paz [c], Rosaria Meli [a], Giuseppina Mattace Raso [a,*]

[a] Department of Pharmacy, School of Medicine, University of Naples "Federico II, 80131 Naples, Italy
[b] Department of Veterinary Medicine and Animal Production, University of Naples "Federico II", 80137 Naples, Italy
[c] University Clinic Hospital of Santiago de Compostela, Santiago de Compostela 15706, Spain

ARTICLE INFO

Keywords:
Chronic kidney disease
Renal fibrosis
N-acylethanolamines
Peroxisome proliferator-activated receptor-α
Epithelial-mesenchymal transition
Extracellular matrix

ABSTRACT

Chronic kidney disease (CKD) development after acute kidney injury (AKI) involves multiple mechanisms, including inflammation, epithelial-mesenchymal transition (EMT), and extracellular matrix deposition, leading to progressive tubulointerstitial fibrosis. Recently, a central role for peroxisome-proliferator activated receptor (PPAR)-α has been addressed in preserving kidney function during AKI. Among endogenous lipid mediators, oleoylethanolamide (OEA), a PPAR-α agonist, has been studied for its metabolic and anti-inflammatory effects. Here, we have investigated OEA effects on folic acid (FA)-induced kidney injury in mice and the underlying mechanisms. OEA improved kidney function, normalized urine output, and reduced serum BUN, creatinine, and albuminuria. Moreover, OEA attenuated tubular epithelial injury, as shown by histological analysis, and decreased expression of neutrophil gelatinase-associated lipocalin and kidney injury molecule-1. Gene expression analysis of kidney tissue indicated that OEA limited immune cell infiltration and inflammation. Moreover, OEA significantly inhibited *Wnt7b* and *Catnb1* gene transcription and α-smooth muscle actin expression, indicating suppression of EMT. Accordingly, OEA exhibited an anti-fibrotic effect, as shown by Masson staining and the reduced levels of transforming growth factor (TGF)-β1, fibronectin, and collagen IV. Mechanistically, the nephroprotective effect of OEA was related to PPAR-α activation since OEA failed to exert its beneficial activity in FA-insulted PPAR-$\alpha^{-/-}$ mice. PPAR-α involvement was also confirmed in HK2 cells where GW6471, a PPAR-α antagonist, blunted OEA activity on the TGF-β1 signalling pathway and associated pro-inflammatory and fibrotic patterns. Our findings revealed that OEA counteracts kidney injury by controlling inflammation and fibrosis, making it an effective therapeutic tool for limiting AKI to CKD progression.

1. Introduction

Acute kidney injury (AKI) is a complex syndrome characterized by a rapid and abrupt reduction of kidney function associated with an increased risk of morbidity and mortality. Following the initial injury, the mechanisms underlying kidney repair could evolve into pathological and maladaptive processes, resulting in chronic inflammation and fibrosis, leading to chronic kidney disease (CKD) [1]. Beyond the underlying cause, AKI is characterized by a certain degree of renal cell death and a strong inflammatory response. In fact, surviving cells undergo a process of dedifferentiation and proliferation to replace damaged cells and restore integrity. De-differentiated epithelial cells, as well as immune cell-derived myofibroblasts, produce pro-fibrotic and inflammatory paracrine factors and are associated with the subsequent

Abbreviations: CKD, Chronic kidney disease; AKI, acute kidney injury; GFR, glomerular filtration rate; PPAR-α, peroxisome proliferator-activated receptor; OEA, oleoyethanolamide; FA, folic acid; EMT, epithelial-mesenchymal transition; ECM, extracellular matrix; TEC, tubular epithelial cell; TGF-β, transforming growth factor; α-SMA, α-smooth muscle cell actin; UACR, urine albumin to creatinine ratio; BUN, Blood urea nitrogen; NAE, N-acyl-ethanolamine; NGAL, neutrophil gelatinase-associated lipocalin; KIM-1, kidney injury molecule; Col4a1, Collagen type IV alpha 1 chain; Fn, Fibronectin; Wnt7b, Wnt family member 7B; Catnb1, catenin beta 1; ERK, extracellular signal-regulated kinase; MAPK, mitogen-activated protein kinase; MCP1, monocyte chemoattractant protein; IFN-γ, interferon.

* Correspondence to: Department of Pharmacy, Via Domenico Montesano, 49, 80131 Naples, Italy.
E-mail address: mattace@unina.it (G. Mattace Raso).

https://doi.org/10.1016/j.biopha.2023.116094
Received 16 October 2023; Received in revised form 22 December 2023; Accepted 26 December 2023
Available online 5 January 2024

development of fibrosis [2,3]. This process recruits infiltrating immune cells that, along with resident ones, foster chronic inflammation, promoting the activation of fibroblasts, which induce extracellular matrix (ECM) deposition and fibrosis [4]. Therefore, preventive and/or therapeutic approaches to counteract the inflammatory and pro-fibrotic response behind kidney damage are ideal potential strategies to limit AKI progression and CKD development. Oleoylethanolamide (OEA) is an endogenous lipid mediator belonging to the N-acyl-ethanolamines (NAEs) family. OEA has been found in different tissues, such as the gastrointestinal tract, muscle, adipocytes, liver, kidney, heart, lung, pancreas, brain, salivary gland, and reproductive tract [5,6]. OEA exhibits multiple actions, mainly as an endogenous peroxisome proliferator-activated receptor (PPAR)-α agonist: in addition to its well-known effect in controlling appetite, lipid metabolism, and body weight, OEA exerts profound anti-inflammatory and analgesic effects [7,8] as well as neuroprotective and anti-atherosclerotic functions [9,10].

Notably, recent findings have indicated that PPAR-α might also play a pivotal role in the molecular control of fibrogenesis; in fact, deletion of PPAR-α worsened renal fibrosis and damage in aged mice [11], whereas moderate exercise upregulated PPAR-α expression, mitigating age-related renal fibrosis in rats [12]. Similarly, the PPAR-α agonists, Wy-14643 and fenofibrate, prevented the development of fibrosis at the hepatic level, as shown in different models of liver injury [13,14].

Animal studies have shown that PPAR-α targeting improves tubular epithelial injury and fibrosis [15]. Indeed, fenofibrate and palmitoylethanolamide, another PPAR-α agonist, have been shown to prevent kidney damage [16–18], as well as pemafibrate has been shown to inhibit renal dysfunction, reducing inflammation and fibrosis in different mouse models of CKD [19].

In the present study, we explored the protective effect of OEA on kidney function and damage on folic acid (FA)-induced renal fibrosis in mice and then examined the underlying molecular mechanisms involved in the progression of AKI toward CKD. This animal model recapitulates the main processes of human AKI and its transition into CKD, i.e., tubular injury, inflammation, and fibrosis and enables kidney function assessment. We have also investigated the contingency of PPAR-α function/activation in OEA beneficial effects *in vivo* by FA challenge of PPAR-$\alpha^{-/-}$ mice and *in vitro* by PPAR-α pharmacological antagonism in TGF-β1-stimulated human proximal tubular epithelial HK-2 cells.

2. Materials and methods

All reagents were obtained from Sigma-Aldrich (USA) unless otherwise stated.

2.1. Animals

Male C57Bl/6 J (Charles River, Wilmington, MA, USA) and PPAR-$\alpha^{-/-}$ (B6.129S4-SvJae-Ppar-atm1Gonz; Jackson Laboratories) mice (21 weeks) weighing approximately 28–30 g were housed in stainless steel cages in a room kept at 22 ± 1°C with a 12:12 h lights-dark cycle (from 7 a.m. to 7 p.m.). Mice were allowed food and water ad libitum. The PPAR-$\alpha^{-/-}$ mice colony was established and maintained by heterozygous crossing. Mice were genotyped as described on the supplier webpage (http://jaxmice.jax.org) using the REDExtract kit (Sigma-Aldrich, Italy).

Animal care and experimental procedures were carried out in compliance with international and national law and policies and approved by the local animal care office (Centro Servizi Veterinari, Università degli Studi di Napoli, Federico II) and the Italian Ministry of Health under protocol no. 1210/2020-PR. Animal studies complied with the Italian DL (No. 26 of 4 March 2014) of the Italian Ministry of Health and the EU Directive 2010/63/EU for animal experiments, ARRIVE guidelines, and the Basel declaration, including the 3Rs concept.

2.2. Experimental setup

Nephropathy was induced chemically with a single intraperitoneal injection of FA (PubChem: CID: 135398656) (Sigma-Aldrich, USA, CAT #F7876) (150 mg/kg) dissolved in 0.3 mol/L sodium bicarbonate. Control mice received sodium bicarbonate alone. OEA was synthesized in the laboratory, as reported in the supplementary material.

The dose of FA was critical for the induction of severe kidney damage and was chosen after preliminary experiments. Unlike many studies in literature performed on 6–8-week-old mice, we used about 5-month-old animals, regarded as mature adult mice, that were more sensitive than young mice to the commonly injected dose of FA. For this reason, a pilot study on the mortality rate following increasing doses of FA was conducted to define the minimum dose required to induce kidney damage without a high rate of mortality (Fig.S1).

Mice were randomly assigned to one of the following groups: (i) control group (CON) receiving vehicle; (ii) control group treated with OEA (2.5 mg/kg/die ip) (CON+OEA); (iii) mice insulted by FA (FA) receiving vehicle; (iv) FA group treated with OEA (FA+OEA, 2.5 mg/kg/day ip). The treatment started 3 days after FA injection and lasted until day 14. This dose was chosen following preliminary experiments to determine the minimally effective pharmacological dose of OEA without excessive weight loss, considering the OEA anorectic effect and the *noticeable body weight loss* due to the FA challenge [20,21]. OEA was dissolved in saline/polyethylene glycol/Tween80 (90/5/5 v/v). Concurrently, PPAR-$\alpha^{-/-}$ mice were divided as follows: (i) control group (PPAR-$\alpha^{-/-}$ CON) receiving vehicle; (ii) PPAR-$\alpha^{-/-}$ mice insulted by FA (150 mg/kg) receiving vehicle (PPAR-$\alpha^{-/-}$ FA) and (iii) FA group treated with OEA (2.5 mg/kg/day ip) (PPAR-$\alpha^{-/-}$ FA+OEA).

Before sacrifice, all mice were placed in individual metabolic cages to evaluate water intake and collect 24-h urine. At the end of the experiment, all mice were anaesthetized with enflurane by inhalation (5% for induction and 3% for maintenance), and blood was taken by intracardiac puncture, after which the animals were euthanized by cervical dislocation. Blood was collected by intracardiac puncture and centrifuged at 2500 rpm at 4 °C for 12 min to obtain the serum samples. Kidneys were removed and snap-frozen for the isolation of RNA or protein or kept in 4% buffered formalin for histological and immunohistochemistry examination.

2.3. Serum and urinary analysis

Urea and creatinine were measured in serum samples. Urea was expressed as BUN (Blood Urea Nitrogen), which was obtained by dividing the urea concentration in the blood by 2.14 (i.e., the ratio between the molecular weight of urea and urea nitrogen). The formula is BUN= [urea]/2.14. All parameters were quantified using commercially available ELISA kits (BioAssay Systems, Hayward, CA) according to the manufacturer's instructions. All samples and standards were analyzed in doublet to avoid intra-test variation. Albumin concentration in urine samples of all groups was analyzed using a mouse albumin ELISA kit (ab108792, Abcam, UK). Albuminuria was also expressed as the ratio of albumin concentration (mg/L) to creatinine concentration (mg/L) in urine. Moreover, urinary indoxyl sulfate (IS) was detected by a mouse IS ELISA kit (Assay Genie, Cat# MOFI01377, Dublin, IE) and the values were expressed in ng/mL.

2.4. Histological score analysis

Kidneys were fixed in 10% neutral-buffered formalin and dehydrated through graded alcohols before being embedded in paraffin wax. Sections were cut at the 5-micron thickness and were stained with hematoxylin–eosin (H&E) or Masson's trichrome. For each case, the percentage of tubules with necrosis, epithelial vacuolization, tubular dilation, and cast formation was evaluated using a 4-point score system as follows: (0) none; (1) < 20%; (2) 20–50%; (3) 50–70%; and (4) >

70%. Similarly, the severity of fibrosis was graded, based on the ratio between fibrosis and total area examined, into the following categories: (0) none; (1) < 20%; (2) 20–50%; (3) 50–70%; and (4) > 70%. The inflammation was graded into the following categories: 0 (absent), 1 (mild inflammation), 2 (moderate inflammation), and 3 (severe inflammation). Each histological section was evaluated by two independent pathologists (G.P. and O.P.; mean work experience of 13 years in the field of veterinary pathology). The differences in the distribution of the semi-quantitative histologic scores among groups were compared using the Kruskal-Wallis and Mann–Whitney U test (IBM SPSS Statistics-Version 25).

2.5. Immunohistochemical examination

Paraffin-embedded samples were sectioned (5 μm thick), dewaxed with xylene, hydrated, and irradiated in a microwave oven (maximum power, 800 W) in trisethylenediamine tetraacetic acid buffer (EDTA; 10 mM Tris base, 1 mM EDTA solution, 0.05% Tween 20) pH 9.0, for 10 min. The peroxidase activity was inhibited by immersing the slides in hydrogen peroxide 0.3% in absolute methanol for 20 min. The sections were incubated overnight at 4 °C with the primary antibody against alfa-SMA. The slides were washed with PBS, then incubated with biotinylated secondary antibody, and labelled with streptavidin-biotin for 30 min at room temperature, followed by incubation with streptavidin conjugated to horseradish peroxidase (LSAB Kit, DakoCytomation, Glostrup, Denmark). The reaction was revealed by diaminobenzidine treatment (DakoCytomation, Denmark), and finally, the sections were counterstained with Mayer's hematoxylin. Approximately five fields at 20x magnification were evaluated for each section. The number of α-SMA positive cells was graded into the following categories: 1 (low number of α-SMA positive cells), 2 (moderate number of α-SMA positive cells), and 3 (high number of α-SMA positive cells). For each sample, five randomly selected fields at 200 × magnification were analyzed in order to obtain a statistically representative evaluation of the whole histological slide. Two independent pathologists (G.P. and O.P.) performed histological analysis with a concordance rate of 98%. The differences in the distribution of the semi-quantitative histologic scores among groups were compared using the Kruskal-Wallis and Mann–Whitney U test (IBM SPSS Statistics-Version 25).

2.6. Cell culture and treatments

The human proximal tubular cell line (HK-2) was obtained from ATCC (CRL-2190™, Manassas, VA). HK-2 cells were grown in DMEM 1.0 g/L glucose (GIBCO, Thermo Fisher Scientific, USA, Cat #31885023) supplemented with 10% FBS (GIBCO, Thermo Fisher Scientific, USA, Cat #10270106), Penicillin-Streptomycin (5000 U/mL) (GIBCO, Thermo Fisher Scientific, USA, Cat #15070063) and maintained at 37 °C in a 5% CO_2 incubator. All cultures used in the experiment were between passages 22 and 30. When cells reached 60–70% of confluence, the medium was replaced with 2% FBS in DMEM. To determine the gene expression of inflammatory and fibrotic markers, after 6-hour starvation, cells were incubated for 24-h with TGF-β1 (10 ng/mL, Sigma-Aldrich Cat #T7039). 12 h before the challenge, cells were pretreated with OEA (5 μM) in the presence or not of PPAR-α antagonist, GW6471 (4 μM) (PubChem CID: 446738) (Tocris Bioscience, UK, cat #4618), added 30 min before OEA. Total RNA was isolated and extracted as reported below.

To better estimate, instead, protein phosphorylation of SMAD3, extracellular signal-regulated kinase (ERK) and p38, the cells were incubated with TGF-β1 (PubChem CID:155011957) (10 ng/mL) for 30 min. One hour before, cells were pretreated with OEA (5 μM) in the presence or absence of GW6471 (4 μM) added for 30 min before OEA. After treatments, cells were collected, and protein lysates were obtained. The results were obtained from three different experiments.

To prepare whole cell lysates, cells were washed with ice-cold phosphate-buffered saline (PBS), harvested, and resuspended in lysis buffer, as reported below. After 1 h, cell lysates were obtained by centrifugation at 20,000 g for 15 min at 4 °C. Protein concentrations were estimated by the Bio-Rad Protein Assay Dye Reagent Concentrate (Bio-Rad Laboratories, USA, Cat #5000006) using bovine serum albumin as standard. For Western blot analysis, protein cell lysate (30 μg) was dissolved in Laemmli sample buffer, boiled for 5 min, and subjected to SDS-PAGE.

2.7. Quantification of gene expression using Real-Time PCR

Total RNA was isolated from the kidney or cells using PureZOL RNA Isolation Reagent (Bio-Rad Laboratories, USA, Cat #7326890) and extracted using a NucleoSpin kit (Macherey-Nagel, DEU), according to the manufacturer's instructions. RNA quality and quantity were determined using a NanoDrop spectrophotometer (Thermo Fisher Scientific, USA). cDNA was obtained using a High-Capacity Reverse Transcription Kit (Thermo Fisher Scientific, USA, Cat #4374966) from 8 μg total RNA from tissue and 3 μg from cells. PCRs were performed with a Bio-Rad CFX96 Connect Real-time PCR System instrument and software. PCR conditions were 15 min at 95 °C followed by 40 cycles of two-step PCR denaturation at 94 °C for 15 s, annealing extension at 55 °C for 30 s and extension at 72 °C for 30 s. Each sample contained 500 ng cDNA in 2X QuantiTect SYBR Green PCR Master Mix (Qiagen, Hilden, Germany, Cat #204145) and primers pairs to amplify Collagen type IV alpha 1 chain (*Col4a1*), Fibronectin 1 (*Fn1*), EGF-like module containing, mucin-like, hormone receptor-like 1 (*Emr1*), also known as F4/80, IL-1β (*Il1b*), IL-6 (*Il6*), tumour necrosis factor-alpha (*Tnf*), interferon-gamma (*Ifng*), chymase 1, mast cell (*Cma1*), tryptase beta-2 (*Tpsb2*), transforming growth factor beta 1 (*Tgfb1*), chemokine (C-C motif) ligand 2 is also referred to as monocyte chemoattractant protein (MCP)1, (*Ccl2*), Wnt family member 7B (*Wnt7b*), Catenin beta 1 (*Catnb1*), kidney injury molecule (KIM)− 1 (*Havcr1*) and neutrophil gelatinase-associated lipocalin (NGAL) (*Lcn2*), and peroxisome proliferator-activated receptor alpha (*Ppara*) (Qiagen, Hilden, Germany) as shown in Table 1, in a final volume of 50 μl. The relative amount of each studied mRNA was normalized to *Gapdh* or *18s* as a housekeeping gene, and data were analyzed according to the $2^{-\Delta\Delta CT}$ method.

2.8. Western blotting

Kidneys were homogenized (Ultra-Turrax T8; IKA Labortechnik, Staufen, Germany) on ice-cold lysis buffer (20 mM Tris–HCl (pH 7.5),

Table 1
Primers for Real-Time PCR.

Genes (Qiagen)	Species	Gene Globe ID	RefSeq Transcript
Catnb1	*Mouse*	QT00160958	NM_001165902
Ccl2	*Mouse*	QT00167832	NM_011333
Cma1	*Mouse*	QT00199465	NM_010780
Col4a1	*Mouse*	QT00100128	NM_009931
Emr1	*Mouse*	QT00099617	NM_010130
Epo	*Mouse*	QT00170331	NM_007942
Fn1	*Mouse*	QT00135758	XM_129845
Gapdh	*Mouse*	QT01658692	NM_008084
Havcr1	*Mouse*	QT00112427	NM_001166631
Ifng	*Mouse*	QT01038821	XM_125899
Il1b	*Mouse*	QT01048355	NM_008361
Il6	*Mouse*	QT00098875	NM_031168
Lcn2	*Mouse*	QT00113407	NM_008491
Ppara	*Mouse*	QT00137984	NM_001113418
Tgfb1	*Mouse*	QT00145250	NM_011577
Tnf	*Mouse*	QT00104006	NM_013693
Tpsb2	*Mouse*	QT00252637	NM_010781
Wnt7b	*Mouse*	QT00168812	NM_009528
18 s	*Human*	QT00000721	X03205
Ccl2	*Human*	QT00212730	NM_002982
Fn1	*Human*	QT00038024	NM_212478
Tnf	*Human*	QT00029162	NM_000594

10 mM NaF, 150 mM NaCl, 1% Nonidet P-40,1 mM phenylmethylsulfonyl fluoride, 1 mM Na_3VO_4, leupeptin and trypsin inhibitor 10 μg/mL; 0.25/50 mg tissue). After 1 h, tissue lysates were obtained by centrifugation at 20,000 g for 15 min at 4 °C. Protein concentrations were estimated by the Bio-Rad protein assay using bovine serum albumin as standard.

Lysates (30 μg) were dissolved in Laemmli sample buffer, boiled for 5 min, separated on SDS-polyacrylamide gel electrophoresis, and transferred to nitrocellulose membrane by TransBlot Turbo (Bio-Rad Technologies, Milan, Italy). The filter was then blocked with 1 × phosphate buffer saline (PBS) and 3% non-fat dried milk for 40 min at room temperature and probed with rabbit polyclonal antibody against phospho-p38 MAPK (Thr180-Tyr182) XP® (1:1000; Cell Signaling cat#4511; Lot:13), p38 MAPK XP® (1:1000; Cell Signaling cat #8690; Lot:9), phospho-p44/42 MAPK (Erk1/2) (Thr202/Tyr204) (1:1000; Cell Signaling Cat #9101; Lot:13), p44/42 MAPK (Erk1/2) (1:1000; Cell Signaling Cat #9102; Lot:28), phospho-Smad3 (Ser423/425) (1:1000; Cell Signaling Cat #9520; Lot:15), Smad3 (1:1000; Cell Signaling Cat #9523; Lot:7) and α-Smooth Muscle Actin XP® (1:1000; Cell Signaling Cat #19245; Lot:3). Western blot for anti-β-actin (1:5000; Sigma-Aldrich Cat #A5441; P60709; Lot:026M4780V) and GAPDH (1:8000; Sigma-Aldrich Cat #G9545; P04406; Lot:127M4814V) were performed to ensure equal sample loading. The filter detection was performed by ChemiDoc Imaging System (Bio-Rad Laboratories, USA).

2.9. Data and statistical analysis

Data were presented as means ± SEM and subjected to one-way variance analysis (ANOVA) for multiple comparisons followed by Bonferroni's post hoc test, using GraphPad Prism 8 (GraphPad Software, San Diego, CA, USA). Differences among groups were considered significant at values of $p < 0.05$.

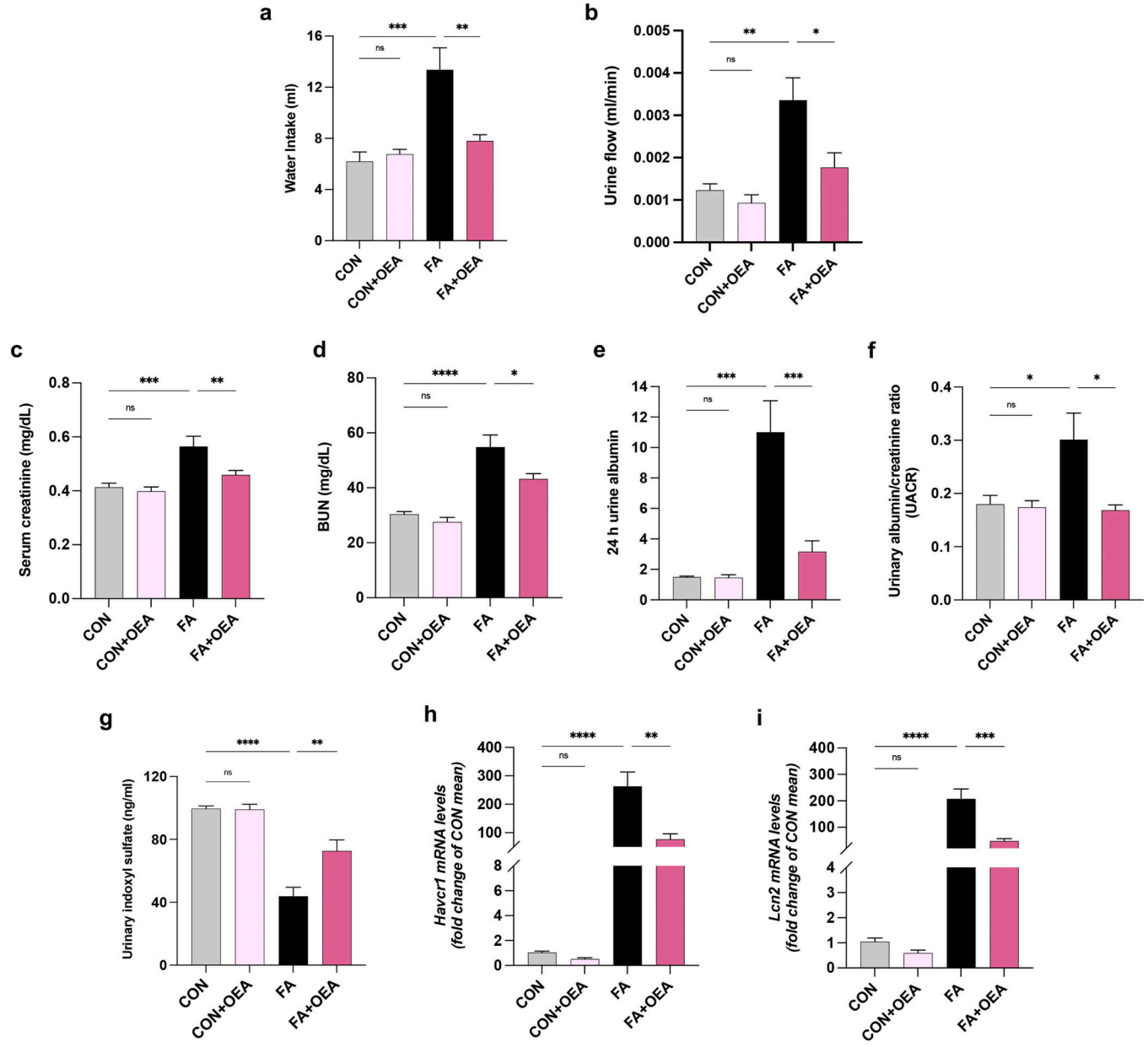

Fig. 1. OEA counteracted kidney dysfunction induced by FA. Water intake (a), urine output (b), serum creatinine (c), BUN (d), 24 h urinary albumin excretion (e), urine albumin to creatinine ratio (UACR) (f) and urinary IS concentration (g) were evaluated 14 days after FA injection. mRNA expression of molecular markers of tubular injury, KIM-1 (h) and NGAL (i) were determined in kidney tissue. Results are shown as mean ± S.E.M (*P < 0,05, **P < 0,01, ***P < 0001 and ****P < 0,0001).

3. Results

3.1. OEA improves kidney function impaired by FA

The ip injection of FA induced a macroscopic reduction in kidney volume that appears visibly restored by OEA treatment (Fig. S2a). However, the experimental groups' kidney-to-body weight ratio remains unchanged (Fig. S2b).

FA challenge caused an increase in water intake and urine excretion, which were normalized in OEA-treated mice (Fig. 1a and b). FA-induced kidney dysfunction was confirmed by the alteration of serum biomarkers, such as creatinine (Cr) and urea, expressed as BUN, that was limited by OEA treatment (Fig. 1c-d). Moreover, the 24-h albumin excretion (Fig. 1e) and urinary albumin/creatinine ratio (Fig. 1f) were significantly reduced in OEA-treated mice compared with the untreated FA-injured group. Notably, urinary indoxyl sulfate concentration, reduced in the FA group, was increased in OEA-treated mice (Fig. 1g). The renoprotective effect of OEA was confirmed by the reduced transcription of tubular injury markers, i.e., KIM-1 (Fig. 1h) and NGAL (Fig. 1i), which were overexpressed in FA-insulted mice.

3.2. OEA limits inflammation induced by FA

To examine the improvement of kidney injury after OEA treatment, we next analyzed hematoxylin and eosin (H&E) staining that showed severe lesions in the tubular epithelial cells (TEC) and interstitium in the kidney from FA mice (Fig. 2a). Statistical analysis showed a significant severe epithelial vacuolization (Fig. 2b), dilation of the tubular lumen (Fig. 2c), cast formation (Fig. 2d), inflammation (Fig. 2e), and necrosis (Fig. 2f) in FA group. In contrast, these alterations were markedly alleviated in mice treated with OEA, as evidenced by the semi-quantitative analysis.

To evaluate the effect of OEA on renal cell recruitment following the FA challenge, we evaluated the transcriptional levels of several markers associated with different inflammatory/immune cell populations. Along with monocyte/macrophage activation, mast cell degranulation is also

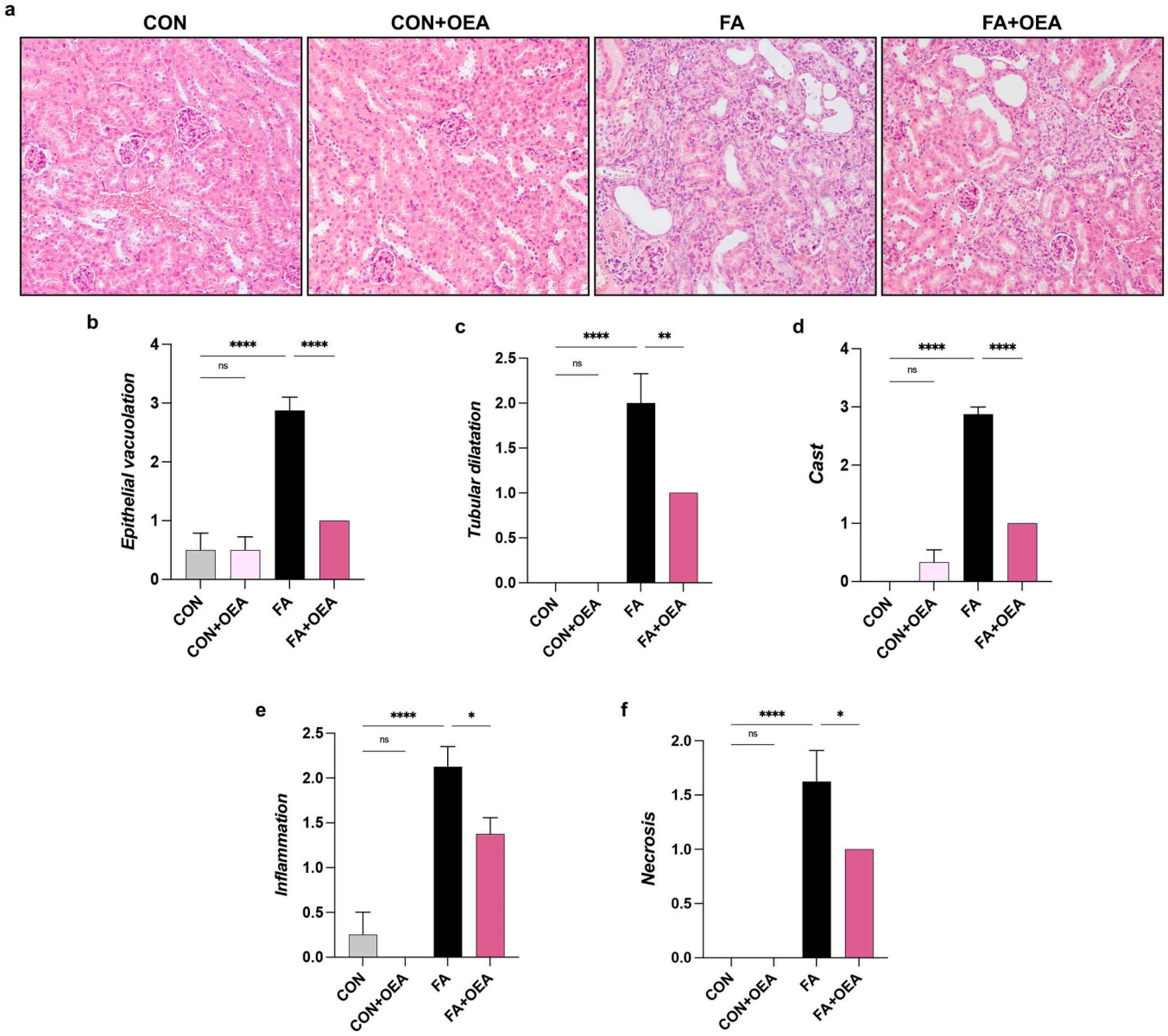

Fig. 2. OEA mitigated pathological renal injury induced by FA. Representative photomicrographs of hematoxylin and eosin (H&E) (a) stained kidney sections (original magnification, 20 ×). The score of epithelial vacuolization (b), tubular dilatation (c), cast (d), inflammation (e) and necrosis (f) were reported. Results are shown as mean ± S.E.M (*P < 0,05, **P < 0,01 and ****P < 0,0001).

involved in the occurrence and progression of renal inflammation and fibrosis [22]. On this basis, beyond *Ccl2* and *Emr1*, we also evaluated the gene transcription of *Cma1* and *Tpsb2*. OEA reduced MCP-1, the macrophage marker F4/80 and at a higher extent, chymase and tryptase, the major constituents of mast cell granules, indicated a reduction of macrophage chemotaxis and infiltration and mast cell activation (Fig. 3a). Therefore, we also evaluated the renal expression of PPAR-α, whose transcriptional activity, along with that of other transcription factors, controls monocyte/macrophage recruitment and the inflammatory process. Notably, the reduced expression of PPAR-α in FA mice was restored by OEA treatment, suggesting a role for this receptor in the OEA effect (Fig. 3b). Finally, OEA attenuated the gene expression of IL-1β, IL-6, TNF-α, IFN-γ, and EPO significantly increased in FA-insulted animals (Fig. 3b).

3.3. OEA suppresses tubulointerstitial fibrosis in FA-challenged mice

Renal fibrosis is a common feature of CKD in which tissue architecture is progressively replaced by ECM proteins, such as fibronectin and collagen IV [3]. As shown by Masson's trichrome staining, OEA treatment significantly reduced the degree of tubulointerstitial fibrosis induced in FA-insulted mice (Fig. 4a). To elucidate the mechanism by which OEA limits renal fibrosis, we have evaluated gene expression abundance of common biomarkers involved in this process. Semi-quantitative PCR showed a significant increase in TGF-β1 in the kidney of FA mice, markedly reduced by OEA treatment (Fig. 4b). Consistently, the increased expression of *Col4a1* and *Fn1*, two major constituents of ECM, in the kidney of FA-insulted animals was significantly inhibited by OEA treatment (Fig. 4c and d). Increasing evidence indicates that sustained activation of Wnt/β-catenin is associated with the development and progression of renal fibrotic lesions by contributing to the epithelial-mesenchymal transition (EMT) [23]. Therefore, the activation of TGF-β1 and Wnt/β-catenin pathways induced the differentiation of several kidney cell types in myofibroblast, expressing α-SMA. Our data showed that OEA treatment reduced the increased levels of *Wnt7b* and *β-catenin-1* mRNAs (Fig. 5a and b), as well as α-SMA expression as shown by IHC and Western blot analysis (Fig. 5c-d).

3.4. PPAR-α involvement in OEA reno-protective effects

PPAR-α involvement in OEA nephroprotective effect was assessed by insulting PPAR-$\alpha^{-/-}$ mice with FA challenge. H&E staining (Fig. 6a) showed mild epithelial vacuolization in the kidney section of PPAR-$\alpha^{-/-}$ control mice than PPAR-$\alpha^{-/-}$ mice insulted by FA, which presented numerous dilated tubules (Fig. 6d) associated with intratubular proteinaceous material (Fig. 6e) and moderate vacuolation (Fig. 6c) which was not reversed in OEA-treated mice. Statistical analysis showed significant severe inflammation (Fig. 6f) and necrosis (Fig. 6g) in FA and FA OEA-treated PPARα$^{-/-}$ mice. Moreover, through Masson's Trichrome (Fig. 6b), we showed the expansion of interstitial connective tissue by fibrous connective tissue (blue) in kidney sections of FA and FA OEA-treated PPAR-$\alpha^{-/-}$ mice associated with the increased fibrosis score (Fig. 6h).

Kidney function was assessed by measuring serum levels of creatinine and BUN. OEA treatment was unable to significantly reduce these markers that were increased in FA-insulted PPAR-$\alpha^{-/-}$ mice (Fig. 7a and b). We evaluated several inflammatory and fibrotic factors to demonstrate PPAR-α involvement in OEA nephroprotective effects further. IL-1β, MCP-1, and F4–80 mRNAs (Fig. 7c) increased upon FA insult in PPAR-$\alpha^{-/-}$ mice and did not significantly change by OEA treatment. Consistently, OEA was also unable to lessen the gene expression of TGF-β1, collagen IV, and fibronectin in FA mice lacking PPAR-α (Fig. 7d).

3.5. OEA reduces TGF-β1 activity by inhibiting the Smad 3/MAP-kinase signalling in HK2 cells

TGF-β1 signalling pathway, the master regulator of fibrosis, was examined in human proximal tubular HK-2 cells to define the direct effect of OEA on tubular cells and to corroborate, as mechanistic insight, the involvement of PPAR-α, through the antagonist GW6471. First, an MTT assay was carried out to determine the appropriate OEA concentration that did not alter cell viability in the presence or not of the profibrotic challenge TGF-β1 (Fig. S3). According to numerous studies [24–27], TGF-β1 (10 ng/mL) induces an EMT in HK-2 cells over a 24-h period [28]. Cell morphology showed that, upon TGF-β1 stimulation, HK-2 cells lost their epithelial appearance and presented elongated and spindle-shaped morphology, attenuated by OEA pretreatment (Fig. S3b). Accordingly, OEA significantly blunted the marked increase in the phosphorylation of SMAD3, p38 and Erk1/2 in TGF-β1-stimulated HK2 cells (Fig. 8A). Nevertheless, the pretreatment with the PPARα-antagonist GW6471 prevented OEA effects. These results confirmed the role of PPAR-α in mediating the damping effect of OEA on TGF-β1 signalling via SMAD and mitogen-activated protein kinase (MAPK) pathway in HK2 cells. Moreover, we showed that GW6471 almost completely abolished the inhibitory effect of OEA of *Ccl2*, *Tnf*, and *Fn1* gene expression in TGF-β1-stimulated tubular cells (Fig. 8B-D). Finally, the reduction of TGF-β1-induced α-SMA expression upon OEA treatment was blunted by PPAR-α blockade (Fig. 8E), indicating a direct suppression of EMT by OEA through a PPAR-α dependent mechanism.

4. Discussion

This study demonstrates the nephroprotective effect of OEA and investigates the underlying mechanisms in the model of renal

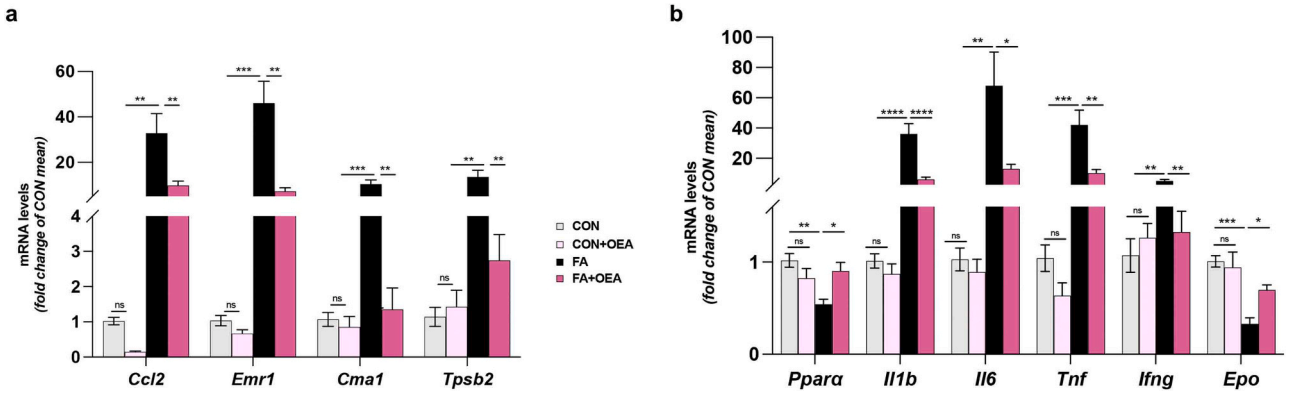

Fig. 3. OEA prevents inflammatory responses induced by FA. Quantitative RT-PCR showed gene expression of *Ccl2*, *Emr1*, *Cma1* and *Tpsb2* in all experimental groups (a). Expression of *Ppara, Il1b, Il6, Tnf*, *Infg*, and *Epo* genes were also shown (b). Results are shown as mean ± S.E.M (*P < 0,05, **P < 0,01, ***P < 0001 and ****P < 0,0001).

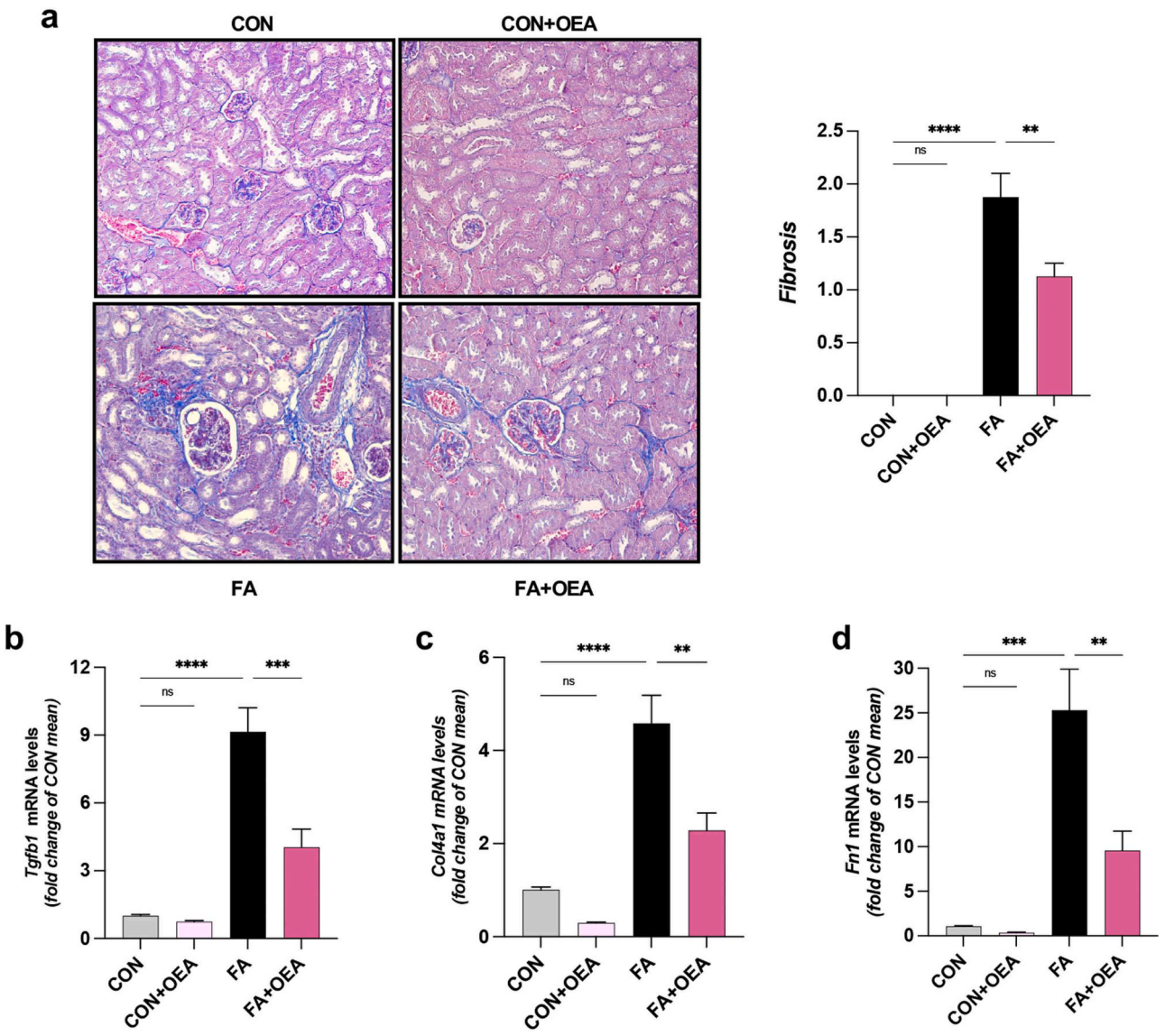

Fig. 4. OEA limits renal fibrotic responses in FA mice. Representative photomicrographs of Masson's trichrome stained kidney sections (original magnification 20 ×) and fibrosis score (a). FA mice showed the renal interstitium moderately expanded by fibrous connective tissue (blue), which was instead attenuated in mice treated with OEA. Renal gene expression of *Tgfb1* (b), *Col4a1* (c) and *Fn1* (d) was assessed by RT-PCR. Results are shown as mean ± S.E.M (**P < 0,01, ***P < 0001 and ****P < 0,0001).

tubulointerstitial fibrosis induced by FA in mice. Moreover, we show that the OEA protective effect is contingent on PPAR-α activation since this acylethanolamide fails to affect FA-insulted PPAR-α deficient mice significantly. This finding is strengthened by *in vitro* studies since the selective PPAR-α antagonist blunts the protective effect evoked by OEA in human epithelial tubular cells following pro-fibrotic challenge.

Many preclinical and clinical findings have indicated the potential of PPAR-α agonists in managing kidney damage associated with metabolic alterations [29]. These investigations were undertaken considering the pivotal pathogenic role of renal lipid accumulation in nephropathies related to obesity, diabetes, and metabolic syndrome. Indeed, PPAR-α regulates lipid metabolism, reducing renal fat accumulation, lipotoxicity, and the resulting inflammation and fibrosis. Moreover, PPAR-α transgenic expression in proximal tubules of mice protected against acute kidney injury [30], while its deficiency worsened the severity of diabetic nephropathy [31]. However, beyond regulating fatty acid metabolism, PPAR-α also controls inflammation through multiple distinct mechanisms, suggesting its pharmacological potential in counteracting metabolic diseases with an inflammatory-related component [32].

Here, we investigate the effect of OEA in a non-metabolic kidney injury model, where the microscopic tubular obstruction by FA crystals is related to a direct toxic effect on TECs, leading to tubular necrosis in the early acute phase, to converge later into interstitial fibrosis. As known, FA-induced kidney damage is a suitable model, covering AKI, CKD, and the AKI to CKD transition [33], since, upon the "early acute phase" occurring within 3 days, the AKI to CKD transition may be investigated due to the progressive renal deterioration, leading to overt CKD 28 days after FA injection [34]. Here, choosing day 14 as an intermediate time point during the progression of CKD, we showed that OEA counteracted the polyurea shown in FA mice, secondary to the reduced capacity to concentrate urines and related to the compensatory increase in water intake. Moreover, OEA ameliorated kidney function, reduced serum creatinine and BUN, and altered albuminuria in FA mice. Notably, OEA treatment also increased IS concentration in urine, which was significantly reduced in FA-insulted mice. The excretion of IS from the blood into the urine, indeed, depends on renal tubule secretion, and its inhibition can cause different degrees of kidney injury and

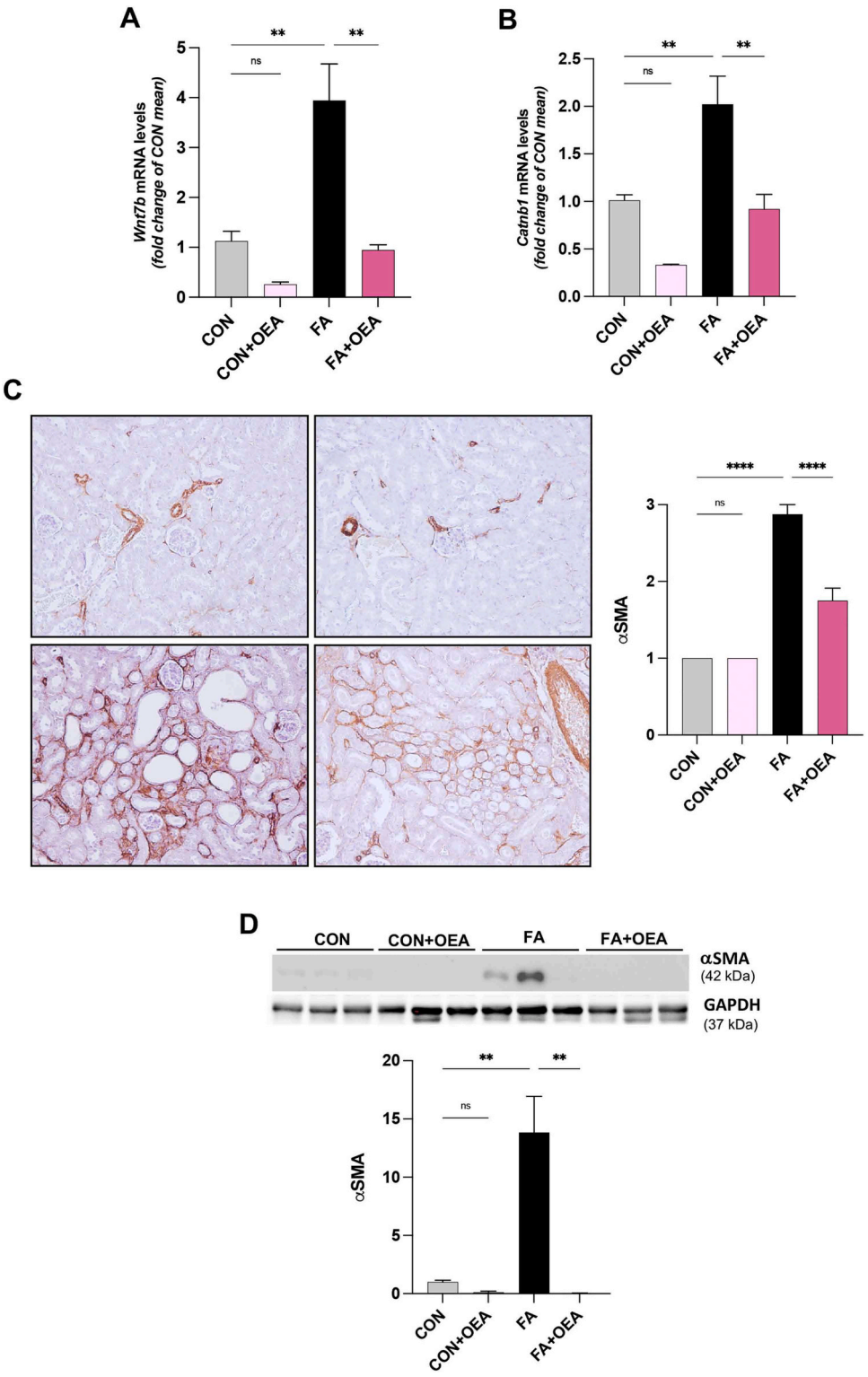

Fig. 5. OEA prevents EMT induced by FA. Gene expression of *Wnt7b* (a) and *β-catenin1* (b) was evaluated by RT-PCR. Myofibroblasts expressed α-smooth muscle cell actin (α-SMA) were evaluated through IHC (c) and protein expressions by Western blot analysis (d). Results are shown as mean ± S.E.M (*P < 0,05 and **P < 0,01).

accelerated CKD development [35]. Consistently, the histological examination of the FA-insulted kidney revealed epithelial vacuolization and tubular dilation, inflammatory cell infiltration, protein casting, and tubular epithelial cell necrosis that was restrained by OEA treatment, indicating a reduction of the extension of tubular damage. These data were consistent with the reduced expression of tubular injury biomarkers, such as KIM-1 and NGAL [36–39]. NGAL is an early prediction marker of AKI expressed in response to urinary obstruction [40]. Although AKI and CKD are recognized as closely linked and regarded as an integrated syndrome [41] involving many common pathological processes [42,43], AKI is mainly characterized by tubulointerstitial injury and tubular cell death, while fibrosis tends to occur under CKD, indicating that AKI is a major risk factor involved in CKD progression [44]. The inflammatory process has been recognized as one of the

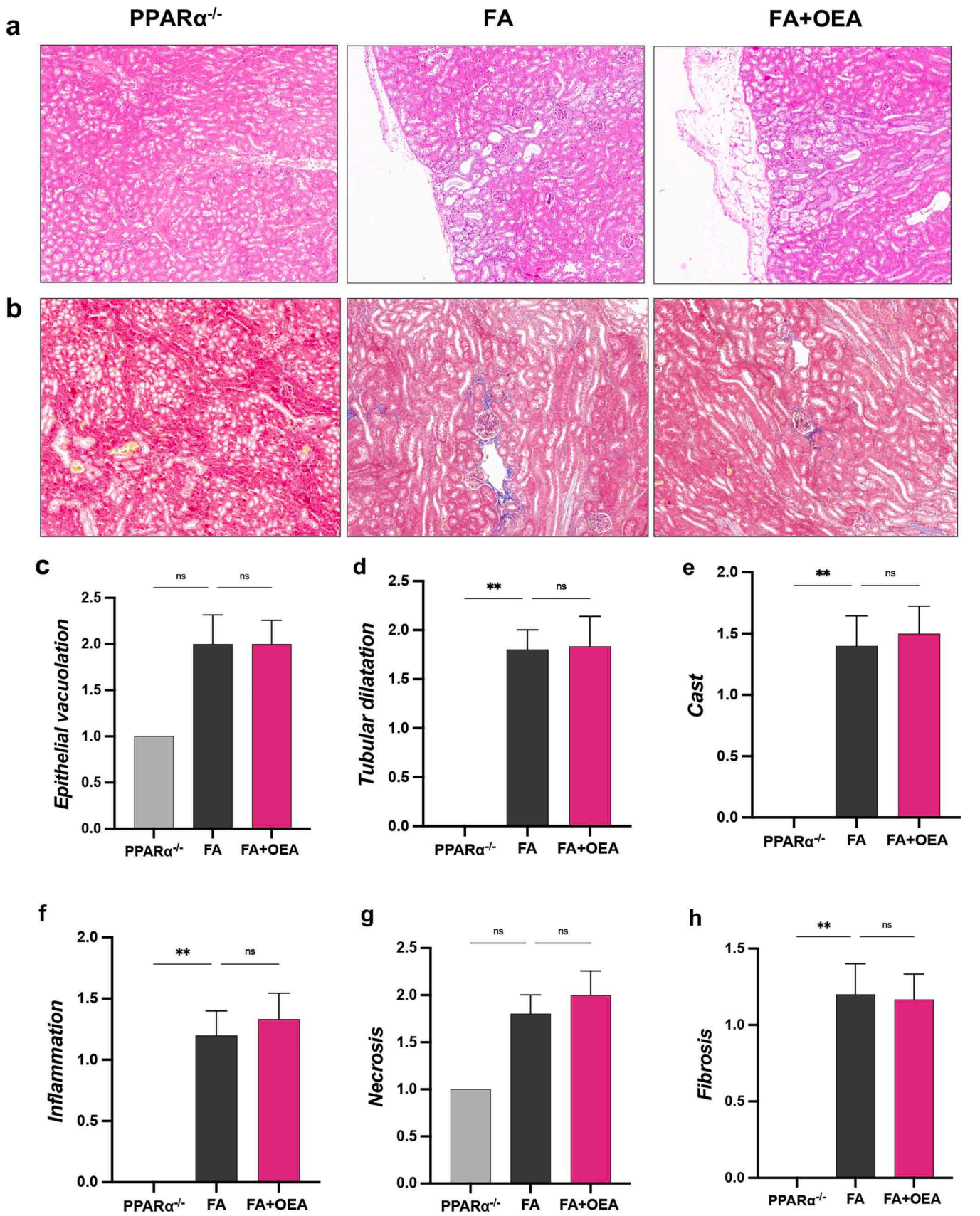

Fig. 6. Renal histological evaluation in OEA-treated PPAR-$\alpha^{-/-}$ mice challenged with FA. Representative photomicrographs of H&E (a) and Masson's trichrome (b) stained kidney sections (original magnification 20 ×) in PPAR-$\alpha^{-/-}$ mice. The score of epithelial vacuolization (c), tubular dilatation (d), cast (e), inflammation (f), necrosis (g) and fibrosis (h) score were reported. Results are shown as mean ± SEM (**P < 0,01).

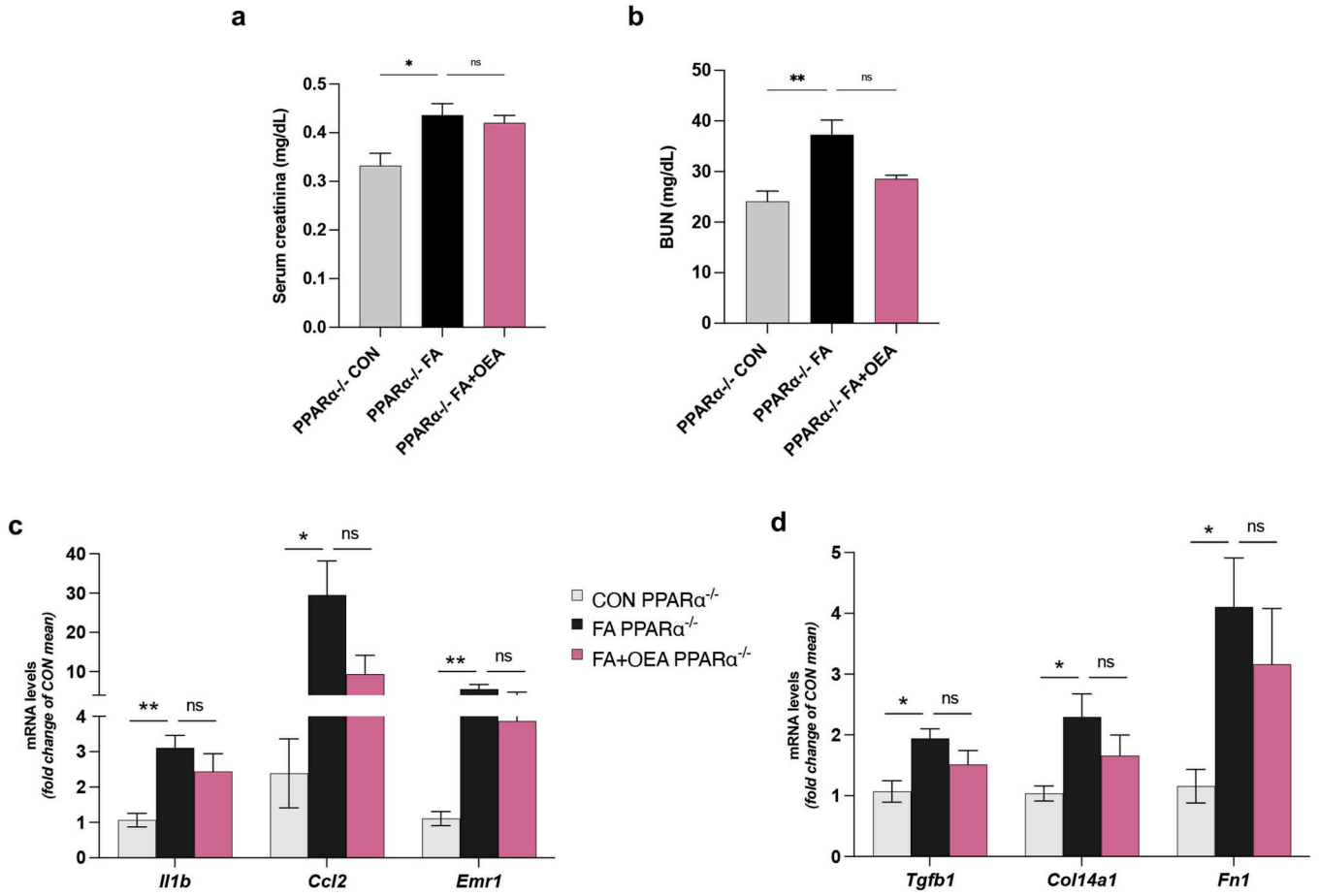

Fig. 7. Ineffectiveness of OEA in FA-insulted PPAR-$\alpha^{-/-}$ mice. Serum creatinine (a) and BUN (b) evaluation in FA-insulted PPAR-$\alpha^{-/-}$ mice treated or not with OEA. Levels of *Il1b*, *Ccl2*, *Emr1* (c) and *Tgfb1*, *Col4a1*, *Fn1* (d) mRNAs were reported. Results were shown as mean ± S.E.M (*P < 0,05 and **P < 0,01).

driving factors involved in the pathogenesis of AKI, playing a key role in the following transition to CKD [45]. Therefore, limiting inflammation-related tubular damage could represent a key strategy for AKI control and worsening and progression into CKD. Here, we showed that OEA attenuates the accumulation of inflammatory cells in the injured kidney, as shown by the expression of several cell markers. OEA reduced *Ccl2* transcription, indicating a reduction in macrophage chemotaxis, which was confirmed by a decrease in F4/80 mRNA levels and mast cell infiltration and activation. A clear role of mastocytes in the early phase of kidney injury has been addressed. Pharmacological intervention targeting mastocytes revealed a protective effect in the renal ischemia-reperfusion injury model in rats, limiting AKI [46].

Afterwards, Danelli et al. [47] studied the role of mastocytes in the acute and chronic phases of kidney injury, indicating a role in disease progression. This study demonstrated that mast cell depletion improved kidney function and reduced local inflammatory cytokine/chemokine levels and neutrophil recruitment in the early acute phase, reducing organ atrophy and fibrosis in the chronic phase [47]. It is conceivable that OEA counteracted the inflammatory response, reducing recruited cells that, along with resident cells, promote cytokine release during kidney injury. Kidney inflammation by FA challenge was associated with PPAR- α reduction in our experimental condition. As known, this nuclear receptor controls the transcription of many inflammatory genes, promoting an anti-inflammatory activity [8,32,48]. The restoration of PPAR-α expression and the downregulation of the transcription of inflammatory cytokines by OEA in FA mice suggested a pivotal role of this receptor in mediating the OEA anti-inflammatory effect. This finding was further supported by the results obtained in PPAR-$\alpha^{-/-}$ mice receiving FA, where OEA treatment failed to preserve kidney morphology and function, being unable to reduce renal inflammation and fibrosis. However, with this premise, the not significant decreasing trend of inflammatory and fibrotic markers by OEA treatment suggests the possible involvement of alternative protective pathways other than those under PPAR-α control. Indeed, unlike other PPAR-α agonists, OEA can also bind to other receptors, i.e. the transient receptor potential vanilloid receptor (TRPV)1 [49] and GPR119 [50]. In particular, TRPV1, localized mainly in sensory neurons, has also been identified in the cortex and medulla of the kidney [51], where its activation by capsaicin has been shown to mitigate ischemia/reperfusion-induced AKI [52]. Therefore, along with the involvement of PPAR-α, the possible contribution of TRPV1 in the renoprotective effect of OEA cannot be excluded.

Notably, OEA significantly limits the fibrotic process, possibly restraining AKI-CKD transition by reducing detrimental inflammatory signals in non-mutated FA-insulted mice. Indeed, we found that OEA treatment markedly blunted the extensive areas of fibrosis shown in FA-challenged mice.

Furthermore, we found a reduced transcription of ECM components, namely fibronectin and collagen IV, in renal tissue from mice treated with OEA. In renal pathophysiology, TGF-β1 expression drives ECM remodeling and expansion of pro-fibrotic cell types, such as fibroblasts and myofibroblasts [53,54], through the de novo synthesis of α-SMA. TGF-β1 has been identified as one of the main inducers of EMT, a pivotal step in the development of renal fibrosis [55–57], where many renal cell types differentiate into myofibroblasts. It has been suggested that damaged TECs inside tubules underwent a "partial" EMT during kidney injury, co-expressing both epithelial and mesenchymal markers. This condition is crucial for intensifying interstitial fibrogenesis since

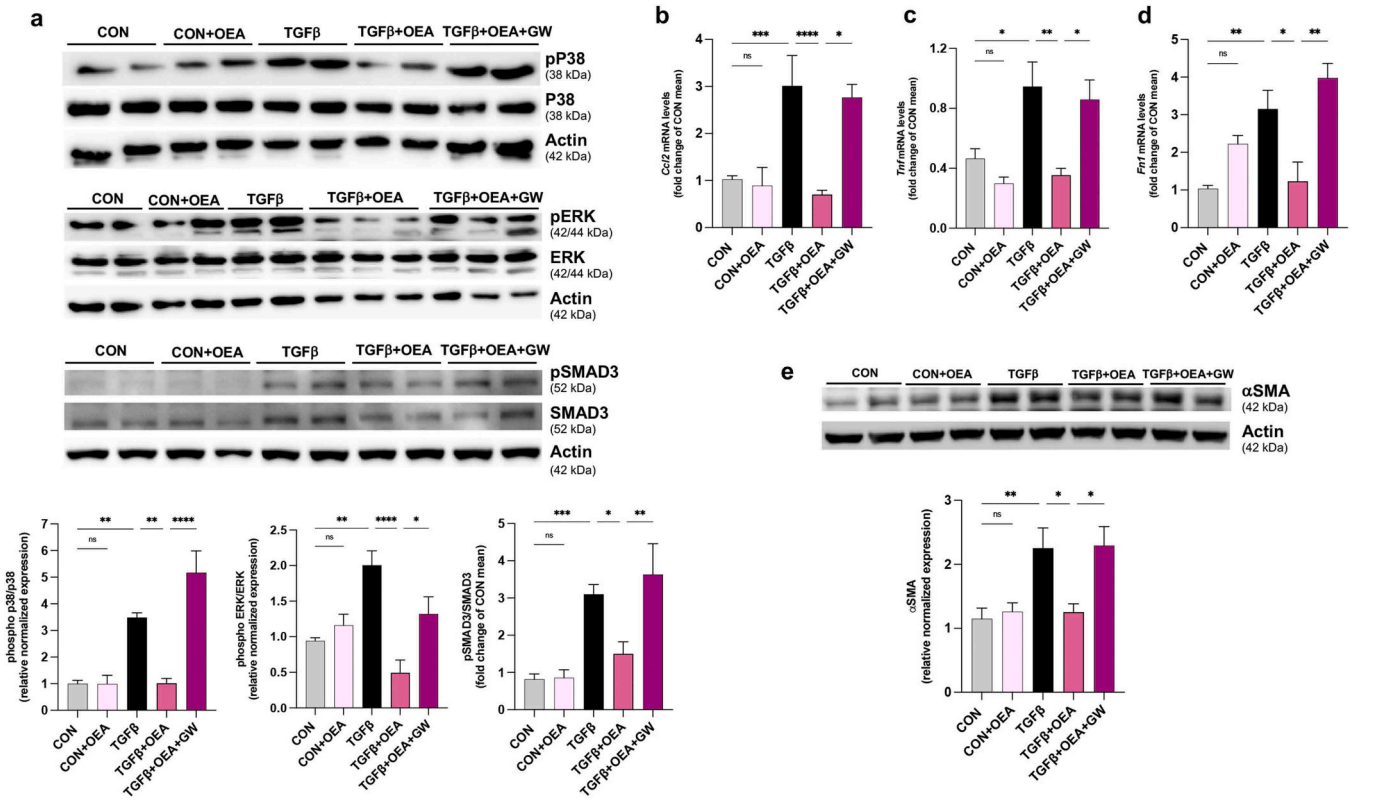

Fig. 8. Effect of OEA on TGFβ1-induced fibrosis in HK2 tubular cells. Representative Western blots of p38, ERK and SMAD3 and the relative phosphorylated and total protein levels were shown (a). Levels of *Ccl2* (b), *Tnf* (c) and *Fn1* (d) mRNA and protein expression of α-SMA (e) were also reported. Stimulation of HK-2 cells with TGFβ-1 (10 ng/mL) after OEA (5 μM) pre-treatment with or without GW-6471 preincubation (4 μM) was performed as reported in Materials and Methods. Results are representative of three replicate experiments. All data are shown as mean ± S.E.M (*P < 0,05, **P < 0,01, ***P < 0001 and ****P < 0,0001).

partially differentiated cells release mediators that can promote myofibroblast differentiation from other renal cell types.

Mechanistically, TGF-β1 signalling can induce the expression of Wnt/β-catenin superfamily members and vice versa, leading to hyperactivation of Wnt/β-catenin signalling in glomeruli and tubulointerstitium associated with the formation of fibroblasts and the development of kidney fibrosis [58,59]. Here, we showed that OEA induced a reduction of renal TGF-β1 expression, affecting its downstream pathways involved in EMT and ECM deposition. Moreover, we showed reduced transcription of renal *Wnt7b* and *Catnb1* genes following OEA treatment. Interestingly, Wnt7b represents a key molecule in the crosstalk between infiltrated macrophages and tubular cells and is implicated in kidney repair and regeneration [60]. Our data indicate that OEA, decreasing α-SMA expression related to a reduction of myofibroblast component, counteracted the maladaptive pathological mechanism of AKI towards CKD.

Of note, TGF-β has recently been shown to downregulate renal EPO expression [61], as well as pro-inflammatory NF-κB signalling and TNF-α transcription [62]. Indeed, anti-inflammatory treatment has been shown to restore EPO production in a UUO model of kidney damage [63]. Very recently, it has been shown that in different animal models of CKD, including FA injection, renal tissue showed decreased *Epo* mRNA levels [64]. It has been hypothesized that, due to the loss of tubular function, oxygen consumption is likely to be decreased in the damaged kidney, leading to "microenvironmental relative hyperoxia", which inhibits hypoxic EPO induction in EPO-producing cells [65,66]. Therefore, it is conceivable that OEA treatment could re-induce EPO expression, possibly reducing the inflammatory and fibrotic process and restoring the physiological oxygen sensing (microenvironmental oxygen partial pressure).

To further elucidate the mechanism by which OEA inhibits the inflammatory process and fibrosis, we examined the direct effect of OEA on the TGF-β1 signalling pathway in HK-2 tubular cells. In *in vitro* studies, we showed that OEA blunted the TGF-β1/SMAD-dependent signalling transduction, reducing the phosphorylation of SMAD3.

On the other hand, OEA also reduced the activation of the non-SMAD signalling pathway related to p38 and ERK1/2 MAPK, inhibiting their TGF-β1-induced phosphorylation. The lower activation of TGF-β1 signalling by OEA resulted in a reduction of both inflammatory and profibrotic responses in tubular cells. Here, we also demonstrated that OEA reduced the TGF-β1-induced α-SMA expression, indicating its capability to limit the EMT of tubular cells. Notably, we have also confirmed the involvement of PPAR-α activation in OEA effects since receptor blockade by the selective antagonist GW6471 blunted OEA anti-inflammatory and anti-fibrotic activity, blocking the activation of TGF-β1 signalling transduction.

In conclusion, OEA treatment exhibits a protective effect in the early stage of FA-induced kidney injury, alleviating inflammation and reducing cell recruitment and cytokine production through a PPAR-α dependent mechanism. Accordingly, OEA could have a long-term beneficial effect against AKI-CKD progression by alleviating inflammation and subsequently limiting fibrosis.

CRediT authorship contribution statement

Melini Stefania: Investigation. **Sodano Federica:** Investigation. **Piegari Giuseppe:** Investigation. **Annunziata Chiara:** Investigation. **Pirozzi Claudio:** Investigation, Writing – review & editing. **Lama Adriano:** Investigation. **Comella Federica:** Investigation, Writing – original draft. **Mattace Raso Giuseppina:** Conceptualization, Funding acquisition, Project administration, Writing – original draft. **Meli Rosaria:** Conceptualization, Methodology, Project administration,

Writing – review & editing. **Lago Paz Francisca:** Funding acquisition, Project administration, Writing – review & editing. **Paciello Orlando:** Writing – review & editing.

Declaration of Competing Interest

The authors declare that they have no known competing financial interests or personal relationships that could have appeared to influence the work reported in this paper.

Acknowledgments

We thank Mr Giovanni Esposito, Mr Angelo Russo, and Dr Antonio Baiano for animal care and technical assistance. Giuseppina Mattace Raso and Rosaria Meli were recipients of the "Programme of International Exchange (2021) between the University of Naples Federico II and Foreign Universities or Research centres for short-term mobility" to collaborate with Francisca Lago Paz (Santiago Clinical Hospital, Santiago de Compostela, Spain).

Funding

This work was partially supported by a grant from POC R&I 2014–2020, Asse tematico I "Capitale Umano"- Azione I.1 "Dottorati innovative con caratterizzazione industriale".

Appendix A. Supporting information

Supplementary data associated with this article can be found in the online version at doi:10.1016/j.biopha.2023.116094.

References

[1] H. Scholz, et al., Kidney physiology and susceptibility to acute kidney injury: implications for renoprotection, Nat. Rev. Nephrol. vol. 17 (fasc. 5) (2021) 335–349, https://doi.org/10.1038/s41581-021-00394-7.
[2] D.A. Ferenbach e, J.V. Bonventre, Mechanisms of maladaptive repair after AKI leading to accelerated kidney ageing and CKD, Nat. Rev. Nephrol. vol. 11 (fasc. 5) (2015) 264–276, https://doi.org/10.1038/nrneph.2015.3.
[3] Y. Liu, Cellular and molecular mechanisms of renal fibrosis, Nat. Rev. Nephrol. vol. 7 (fasc. 12) (2011) 684–696, https://doi.org/10.1038/nrneph.2011.149.
[4] M. Zeisberg, e E.G. Neilson, Mechanisms of tubulointerstitial fibrosis, J. Am. Soc. Nephrol. vol. 21 (fasc. 11) (2010) 1819–1834, https://doi.org/10.1681/ASN.2010080793.
[5] A. Ambrosini, et al., Oleoylethanolamide protects human sperm cells from oxidation stress: studies on cases of idiopathic infertility1, Biol. Reprod. vol. 74 (fasc. 4) (2006) 659–665, https://doi.org/10.1095/biolreprod.105.046060.
[6] H. Tutunchi, M. Saghafi-Asl, e A. Ostadrahimi, A systematic review of the effects of oleoylethanolamide, a high-affinity endogenous ligand of PPAR-α, on the management and prevention of obesity, Clin. Exp. Pharm. Physiol. vol. 47 (fasc. 4) (2020) 543–552, https://doi.org/10.1111/1440-1681.13238.
[7] L. Yang, et al., Oleoylethanolamide exerts anti-inflammatory effects on LPS-induced THP-1 cells by enhancing PPARα signaling and inhibiting the NF-κB and ERK1/2/AP-1/STAT3 pathways, Sci. Rep. vol. 6 (fasc. 1) (2016) 34611, https://doi.org/10.1038/srep34611.
[8] S. Pontis, A. Ribeiro, O. Sasso, e D. Piomelli, Macrophage-derived lipid agonists of PPAR- α as intrinsic controllers of inflammation, Crit. Rev. Biochem. Mol. Biol. vol. 51 (fasc. 1) (2016) 7–14, https://doi.org/10.3109/10409238.2015.1092944.
[9] A. Fan, et al., Atheroprotective Effect of Oleoylethanolamide (OEA) targeting oxidized LDL, PLoS ONE vol. 9 (fasc. 1) (2014) e85337, https://doi.org/10.1371/journal.pone.0085337.
[10] R. Gonzalez-Aparicio, et al., The systemic administration of oleoylethanolamide exerts neuroprotection of the nigrostriatal system in experimental Parkinsonism, Int. J. Neuropsychopharm. vol. 17 (fasc. 03) (2014) 455–468, https://doi.org/10.1017/S1461145713001259.
[11] K.W. Chung, E.K. Lee, M.K. Lee, G.T. Oh, B.P. Yu, e H.Y. Chung, Impairment of PPARα and the fatty acid oxidation pathway aggravates renal fibrosis during aging, JASN vol. 29 (fasc. 4) (2018) 1223–1237, https://doi.org/10.1681/ASN.2017070802.
[12] H.-X. Zhao, Z. Zhang, F. Hu, Q.-F. Wei, Y.-S. Yu, e H.-D. Zhao, Swimming exercise activates peroxisome proliferator-activated receptor-alpha and mitigates age-related renal fibrosis in rats, Mol. Cell Biochem vol. 478 (fasc. 5) (2023) 1109–1116, https://doi.org/10.1007/s11010-022-04581-3.
[13] E. Ip, G. Farrell, P. Hall, G. Robertson, e I. Leclercq, Administration of the potent PPAR? agonist, Wy-14,643, reverses nutritional fibrosis and steatohepatitis in mice, Hepatology vol. 39 (fasc. 5) (2004) 1286–1296, https://doi.org/10.1002/hep.20170.
[14] T. Toyama, et al., PPARα ligands activate antioxidant enzymes and suppress hepatic fibrosis in rats, Biochem. Biophys. Res. Commun. vol. 324 (fasc. 2) (2004) 697–704, https://doi.org/10.1016/j.bbrc.2004.09.110.
[15] H.M. Kang, et al., Defective fatty acid oxidation in renal tubular epithelial cells has a key role in kidney fibrosis development, Nat. Med vol. 21 (fasc. 1) (2015) 37–46, https://doi.org/10.1038/nm.3762.
[16] E.N. Kim, et al., PPARα agonist, fenofibrate, ameliorates age-related renal injury, Exp. Gerontol. vol. 81 (2016) 42–50, https://doi.org/10.1016/j.exger.2016.04.021.
[17] Y. Wang, L. Pang, Y. Zhang, J. Lin, e H. Zhou, Fenofibrate improved interstitial fibrosis of renal allograft through inhibited epithelial-mesenchymal transition induced by oxidative stress, Oxid. Med. Cell. Longev. vol. (2019) 1–12, https://doi.org/10.1155/2019/8936856.
[18] G. Mattace Raso, et al., Palmitoylethanolamide treatment reduces blood pressure in spontaneously hypertensive rats: involvement of Cytochrome P450-derived eicosanoids and renin angiotensin system, PLoS ONE vol. 10 (fasc. 5) (2015) e0123602, https://doi.org/10.1371/journal.pone.0123602.
[19] Y. Horinouchi, et al., Pemafibrate inhibited renal dysfunction and fibrosis in a mouse model of adenine-induced chronic kidney disease, Life Sci. vol. 321 (2023) 121590, https://doi.org/10.1016/j.lfs.2023.121590.
[20] Mullin E.M., Bonar R.A., Paulson D.F., Acute tubular necrosis. An experimental model detailing the biochemical events accompanying renal injury and recovery, 1976.
[21] P. Laleh, K. Yaser, e O. Alireza, Oleoylethanolamide: a novel pharmaceutical agent in the management of obesity-an updated review, J. Cell. Physiol. vol. 234 (fasc. 6) (2019) 7893–7902, https://doi.org/10.1002/jcp.27913.
[22] M. Jiang, et al., Combined Blockade of Smad3 and JNK Pathways Ameliorates Progressive Fibrosis in Folic Acid Nephropathy, Front. Pharmacol. vol. 10 (2019) 880, https://doi.org/10.3389/fphar.2019.00880.
[23] S.J. Schunk, J. Floege, D. Fliser, e T. Speer, WNT–β-catenin signalling — a versatile player in kidney injury and repair, Nat. Rev. Nephrol. vol. 17 (fasc. 3) (2021) 172–184, https://doi.org/10.1038/s41581-020-00343-w.
[24] X. Geng, et al., Ganoderic acid hinders renal fibrosis via suppressing the TGF-β/Smad and MAPK signaling pathways, Acta Pharm. Sin. vol. 41 (fasc. 5) (2020) 670–677, https://doi.org/10.1038/s41401-019-0324-7.
[25] R. Li, Y. Guo, Y. Zhang, X. Zhang, L. Zhu, e T. Yan, Salidroside ameliorates renal interstitial fibrosis by inhibiting the TLR4/NF-κB and MAPK signaling pathways, IJMS vol. 20 (fasc. 5) (2019) 1103, https://doi.org/10.3390/ijms20051103.
[26] Z. Sun, Y. Ma, F. Chen, S. Wang, B. Chen, e J. Shi, miR-133b and miR-199b knockdown attenuate TGF-β1-induced epithelial to mesenchymal transition and renal fibrosis by targeting SIRT1 in diabetic nephropathy, Eur. J. Pharmacol. vol. 837 (2018) 96–104, https://doi.org/10.1016/j.ejphar.2018.08.022.
[27] J. Wang, et al., Nrf2 signaling attenuates epithelial-to-mesenchymal transition and renal interstitial fibrosis via PI3K/Akt signaling pathways, Exp. Mol. Pathol. vol. 111 (2019) 104296, https://doi.org/10.1016/j.yexmp.2019.104296.
[28] M. Tang, et al., Celastrol alleviates renal fibrosis by upregulating cannabinoid receptor 2 expression, Cell Death Dis. vol. 9 (fasc. 6) (2018) 601, https://doi.org/10.1038/s41419-018-0666-y.
[29] P. Balakumar, S. Kadian, e N. Mahadevan, Are PPAR alpha agonists a rational therapeutic strategy for preventing abnormalities of the diabetic kidney? Pharmacol. Res. vol. 65 (fasc. 4) (. 2012) 430–436, https://doi.org/10.1016/j.phrs.2012.01.004.
[30] S. Li, et al., Transgenic expression of proximal tubule peroxisome proliferator–activated receptor-α in mice confers protection during acute kidney injury, Kidney Int. vol. 76 (fasc. 10) (2009) 1049–1062, https://doi.org/10.1038/ki.2009.330.
[31] C.W. Park, et al., Accelerated diabetic nephropathy in mice lacking the peroxisome proliferator–activated receptor α, Diabetes vol. 55 (fasc. 4) (. 2006) 885–893, https://doi.org/10.2337/diabetes.55.04.06.db05-1329.
[32] N. Bougarne, et al., Molecular actions of PPARα in lipid metabolism and inflammation, Endocr. Rev. vol. 39 (fasc. 5) (2018) 760–802, https://doi.org/10.1210/er.2018-00064.
[33] M.M. Perales-Quintana, et al., Metabolomic and biochemical characterization of a new model of the transition of acute kidney injury to chronic kidney disease induced by folic acid, PeerJ vol. 7 (2019) e7113, https://doi.org/10.7717/peerj.7113.
[34] O.E. Aparicio-Trejo, et al., Chronic impairment of mitochondrial bioenergetics and β-oxidation promotes experimental AKI-to-CKD transition induced by folic acid, Free Radic. Biol. Med vol. 154 (2020) 18–32, https://doi.org/10.1016/j.freeradbiomed.2020.04.016.
[35] K.T. Bush, P. Singh, e S.K. Nigam, Gut-derived uremic toxin handling in vivo requires OAT-mediated tubular secretion in chronic kidney disease, e133817, 133817, JCI Insight vol. 5 (fasc. 7) (2020), https://doi.org/10.1172/jci.insight.133817.
[36] B. Desanti De Oliveira, et al., Molecular nephrology: types of acute tubular injury, Nat. Rev. Nephrol. vol. 15 (fasc. 10) (2019) 599–612, https://doi.org/10.1038/s41581-019-0184-x.
[37] V.S. Vaidya, e J.V. Bonventre, Mechanistic biomarkers for cytotoxic acute kidney injury, Expert Opin. Drug Metab. Toxicol. vol. 2 (fasc. 5) (2006) 697–713, https://doi.org/10.1517/17425255.2.5.697.
[38] P.L. Zhang, L.I. Rothblum, W.K. Han, T.M. Blasick, S. Potdar, e J.V. Bonventre, Kidney injury molecule-1 expression in transplant biopsies is a sensitive measure of cell injury, Kidney Int. vol. 73 (fasc. 5) (2008) 608–614, https://doi.org/10.1038/sj.ki.5002697.

[39] V.S. Sabbisetti, K. Ito, C. Wang, L. Yang, S.C. Mefferd, e J.V. Bonventre, Novel assays for detection of urinary KIM-1 in mouse models of kidney injury, Toxicol. Sci. vol. 131 (fasc. 1) (2013) 13–25, https://doi.org/10.1093/toxsci/kfs268.
[40] D. Kostic, et al., The role of renal biomarkers to predict the need of surgery in congenital urinary tract obstruction in infants, J. Pediatr. Urol. vol. 15 (fasc. 3) (2019) 242.e1–242.e9, https://doi.org/10.1016/j.jpurol.2019.03.009.
[41] L.S. Chawla, e P.L. Kimmel, Acute kidney injury and chronic kidney disease: an integrated clinical syndrome, Kidney Int. vol. 82 (fasc. 5) (2012) 516–524, https://doi.org/10.1038/ki.2012.208.
[42] M. Andreucci, T. Faga, A. Pisani, M. Perticone, e A. Michael, The ischemic/nephrotoxic acute kidney injury and the use of renal biomarkers in clinical practice, Eur. J. Intern. Med. vol. 39 (2017) 1–8, https://doi.org/10.1016/j.ejim.2016.12.001.
[43] Z.H. Endre, J.W. Pickering, e R.J. Walker, Clearance and beyond: the complementary roles of GFR measurement and injury biomarkers in acute kidney injury (AKI), Am. J. Physiol. -Ren. Physiol. vol. 301 (fasc. 4) (2011) F697–F707, https://doi.org/10.1152/ajprenal.00448.2010.
[44] N. Pannu, Bidirectional relationships between acute kidney injury and chronic kidney disease, Curr. Opin. Nephrol. Hypertens. vol. 22 (fasc. 3) (2013) 351–356, https://doi.org/10.1097/MNH.0b013e32835fe5c5.
[45] Y. Sato, M. Takahashi, e M. Yanagita, Pathophysiology of AKI to CKD progression, Semin. Nephrol. vol. 40 (fasc. 2) (2020) 206–215, https://doi.org/10.1016/j.semnephrol.2020.01.011.
[46] F. Tong, L. Luo, e D. Liu, Effect of Intervention in Mast Cell Function Before Reperfusion on Renal Ischemia-Reperfusion Injury in Rats, Kidney Blood Press Res vol. 41 (fasc. 3) (2016) 335–344, https://doi.org/10.1159/000443437.
[47] L. Danelli, et al., Early phase mast cell activation determines the chronic outcome of renal ischemia–reperfusion injury, J. Immunol. vol. 198 (fasc. 6) (2017) 2374–2382, https://doi.org/10.4049/jimmunol.1601282.
[48] M. Grabacka, M. Pierzchalska, P.M. Płonka, e P. Pierzchalski, The role of PPAR alpha in the modulation of innate immunity, IJMS vol. 22 (fasc. 19) (2021) 10545, https://doi.org/10.3390/ijms221910545.
[49] G.P. Ahern, Activation of TRPV1 by the satiety factor oleoylethanolamide, J. Biol. Chem. vol. 278 (fasc. 33) (2003) 30429–30434, https://doi.org/10.1074/jbc.M305051200.
[50] L.M. Lauffer, R. Iakoubov, e P.L. Brubaker, GPR119 is essential for oleoylethanolamide-induced glucagon-like peptide-1 secretion from the intestinal enteroendocrine L-cell, Diabetes vol. 58 (fasc. 5) (2009) 1058–1066, https://doi.org/10.2337/db08-1237.
[51] J.F. Sanchez, J.E. Krause, e D.N. Cortright, The distribution and regulation of vanilloid receptor VR1 and VR1 5′ splice variant RNA expression in rat, Neuroscience vol. 107 (fasc. fasc. 3) (2001) 373–381, https://doi.org/10.1016/s0306-4522(01)00373-6.
[52] K. Ueda, F. Tsuji, T. Hirata, M. Takaoka, e Y. Matsumura, Preventive effect of TRPV1 agonists capsaicin and resiniferatoxin on ischemia/reperfusion-induced renal injury in rats, J. Cardiovasc Pharm. vol. 51 (fasc. 5) (2008) 513–520, https://doi.org/10.1097/FJC.0b013e31816f6884.
[53] N.G. Frangogiannis, Transforming growth factor–β in tissue fibrosis, J. Exp. Med. vol. 217 (fasc. 3) (2020) e20190103, https://doi.org/10.1084/jem.20190103.
[54] A. Sebe, et al., Transforming growth factor- -induced alpha-smooth muscle cell actin expression in renal proximal tubular cells is regulated by p38 mitogen-activated protein kinase, extracellular signal-regulated protein kinase1,2 and the Smad signalling during epithelial-myofibroblast transdifferentiation, Nephrol. Dial. Transplant. vol. 23 (fasc. 5) (2008) 1537–1545, https://doi.org/10.1093/ndt/gfm789.
[55] Q. Xiao, Y. Guan, C. Li, L. Liu, D. Zhao, e H. Wang, Decreased expression of transforming growth factor-β1 and α-smooth muscle actin contributes to the protection of lotensin against chronic renal failure in rats, Ren. Fail. vol. 40 (fasc. 1) (2018) 583–589, https://doi.org/10.1080/0886022X.2018.1496934.
[56] P.C.-T. Tang, et al., TGF-β1 signaling: immune dynamics of chronic kidney diseases, Front. Med. vol. 8 (2021) 628519, https://doi.org/10.3389/fmed.2021.628519.
[57] M. Gwon, et al., Anti-fibrotic effects of synthetic TGF-β1 and Smad oligodeoxynucleotide on kidney fibrosis in vivo and in vitro through inhibition of both epithelial dedifferentiation and endothelial-mesenchymal transitions, FASEB J. vol. 34 (fasc. 1) (2020) 333–349, https://doi.org/10.1096/fj.201901307RR.
[58] W. He, C. Dai, Y. Li, G. Zeng, S.P. Monga, e Y. Liu, Wnt/β-catenin signaling promotes renal interstitial fibrosis, J. Am. Soc. Nephrol. vol. 20 (fasc. 4) (2009) 765–776, https://doi.org/10.1681/ASN.2008060566.
[59] Q. Guo, et al., Protective or deleterious role of Wnt/beta-catenin signaling in diabetic nephropathy: an unresolved issue, Pharmacol. Res. vol. 144 (2019) 151–157, https://doi.org/10.1016/j.phrs.2019.03.022.
[60] S.-L. Lin, et al., Macrophage Wnt7b is critical for kidney repair and regeneration, Proc. Natl. Acad. Sci. U. S. A. vol. 107 (fasc. 9) (2010) 4194–4199, https://doi.org/10.1073/pnas.0912228107.
[61] H.-M. Shih, et al., Transforming growth factor-β1 decreases erythropoietin production through repressing hypoxia-inducible factor 2α in erythropoietin-producing cells, J. Biomed. Sci. vol. 28 (fasc. 1) (2021) 73, https://doi.org/10.1186/s12929-021-00770-2.
[62] S. Imagawa, et al., A GATA-specific inhibitor (K-7174) rescues anemia induced by IL-1beta, TNF-alpha, or L-NMMA, FASEB J. vol. 17 (fasc. 12) (2003) 1742–1744, https://doi.org/10.1096/fj.02-1134fje.
[63] T. Souma, et al., Plasticity of renal erythropoietin-producing cells governs fibrosis, J. Am. Soc. Nephrol. vol. 24 (fasc. 10) (2013) 1599–1616, https://doi.org/10.1681/ASN.2013010030.
[64] G.R. Estrela, et al., Chronic kidney disease induced by cisplatin, folic acid and renal ischemia reperfusion induces anemia and promotes GATA-2 activation in mice, Biomedicines vol. 9 (fasc. 7) (2021) 769, https://doi.org/10.3390/biomedicines9070769.
[65] K.U. Eckardt, A. Kurtz, e C. Bauer, Regulation of erythropoietin production is related to proximal tubular function, Pt 2, Am. J. Physiol. vol. 256 (fasc. 5) (1989) F942–947, https://doi.org/10.1152/ajprenal.1989.256.5.F942.
[66] S.L. Dahl, A.M. Bapst, S.N. Khodo, C.C. Scholz, e R.H. Wenger, Fount, fate, features, and function of renal erythropoietin-producing cells, Pflug. Arch. vol. 474 (fasc. 8) (2022) 783–797, https://doi.org/10.1007/s00424-022-02714-7.